Estimating Dark Matter Coupling Strength in GPS Atomic Clocks for Multiple Events

Author:

Trevor Maddox

Supervisor:

Andrei Derevianko

A thesis presented for the degree of

Bachelor of Science in Physics

Department of Physics

University of Nevada, Reno

December 14, 2020

Abstract

The GPS.DM group works to find dark matter using the GPS satellite constellation. Should a dark matter object, of some shape, pass through a satellite, it may feebly interact with atomic clocks on board, briefly changing the clock frequency. To test this hypothesis, the group takes time data from the Jet Propulsion Laboratory and analyzes it for variations in apparent time between satellite clocks and a reference clock. Here I expand upon the Bayesian statistical analysis used in previous work to estimate the strength of these interactions. I work with a set of multiple time windows and combine them such that a total posterior probability is generated. This total posterior probability contains information about the event magnitude of a time window versus surrounding windows. This method increases the network sensitivity in proportion to the square root of number of windows used.

Contents

List of Figures

List of Tables

Chapter 1

Introduction

The existence of dark matter (DM) in the universe is well known, but its exact nature remains elusive. While DM is commonly observed at galactic scale in examples such as galactic rotation curves, gravitational lensing, and structure formations, [1] there is yet to be extrapolation to laboratory scales [2]. Experiments to detect DM at terrestrial scale are regularly proposed [3] and call for extremely sensitive detection. However, directly detecting DM is problematic by virtue of the unknown nature of its constituents.

Indirect detection is often proposed instead, which attempts to find secondary effects caused by DM. Many models are proposed in indirect detection of DM, but of interest here is the model of ultralight fields such as axions [4]. Ultralight fields may form stable topological defects (TDs) such as monopoles, strings, or domain walls [5]. Detecting these fields directly is not achievable for the hypothesized mass ($m \sim 10^{-23}eV$) so instead experiments to detect their produced phenomenology are proposed [1]. Examples include using ground-based gravitational-wave interferometers [6], accounting for plasma effects with a photon [7], or using pulsar timing arrays [1].

Direct detection is hypothetically plausible for large scale detectors, such as the case here where we use the GPS constellation as the detector. This allows us to assume the fields' masses are at a much higher scale comparable to other

direct detection experiments. This is only possible so long as the DM object is a macroscopic field such as a topological defect [8].

Topological defects (TDs) may be formed during the cooling of the early universe through a spontaneous symmetry breaking phase transition [9, 10]. Searches for TDs have been performed via their gravitational effects, including gravitational lensing. Limits on TDs have been placed by Planck and BICEP2 from fluctuations in the microwave background. The past several years have brought proposals for TD searches via their *non*-gravitational signatures [5]. Here we focus on the non-gravitational interactions to detect TDs as DM passing through GPS satellites.

GPS satellites track time with on-board atomic clocks. Using the data publicly available from the Jet Propulsion Laboratory (JPL), we can analyze the time as measured by said clocks to search for DM-induced transient variations of fundamental constants [5, 8]. Specifically, we track the time differences between a network of satellite and station clocks. In effect this makes the GPS satellite constellation a ∼50,000 km-aperture DM detector. For an Earth-sized object the mass scale is $\sim 10^{-14} eV$ which is in line with other DM searches [5].

Chapter 2

Clumpy Dark Matter Models

Macroscopic objects may form from ultralight DM fields due to self-interaction in the dark sector. TD's are an example of such "clumpy" objects which may also take various dimensionalities such as monopoles (0D), strings (1D), or domain walls (2D). Other examples of macroscopic DM candidates include Q-balls, solitons, and axion stars, but for concreteness we are focusing on topological defects.

Inside the defect, the amplitude of the DM field A and the average energy density of the defect is related by $\rho_{\text{inside}} = A^2/(\hbar c d^2)$ where d is the width or spatial scope of the defect (we use the convention where the field has units of energy) [8]. The DM object width d is treated as a free observational parameter and, for TD models, may be linked to the mass of the DM field particles m_ϕ through the healing length which is on the order of the Compton wavelength $d = \hbar/(m_\phi c)$. Local DM energy density can be described by A and d by assuming that the defects saturate the local DM energy density,

$$A^2 = (\hbar c)\rho_{DM} d^2 \frac{\mathcal{T}}{\tau_{\text{avg}}}, \tag{2.1}$$

where $\tau_{\text{avg}} \sim d/v_g$ is the average duration of the object crossing through a

point-like instrument and $\mathcal{T}$ is the average time between subsequent DM objects with the device [5]. Local dark matter density $\rho_{\rm DM} \approx 0.4\,{\rm GeV\,cm^{-3}}$ is taken from direct measurements and relative velocities of TD objects $v_g \sim 300\,{\rm km\,s^{-1}}$ according to the standard halo model.

As per previous work of GPS.DM [11], we assume a quadratic scalar portal to describe non-gravitational interactions,

$$-\mathcal{L}_{int} = \left(\Gamma_f m_f c^2 \overline{\psi}_f \psi_f + \Gamma_\alpha \frac{F_{\mu\eta}^2}{4} + \dots \right) \phi\phi^*, \tag{2.2}$$

where m_f are fermion masses, ϕ is the scalar DM field (in units of energy), Γ_X are coupling constants to quantify the DM interaction strength, and ψ_f and $F_{\mu\eta}$ are the standard model fermion fields and the electromagnetic Faraday tensor, respectively. The index representing standard model fermions, f, from above equation are implicitly summed over. The Lagrangian leads to redefinitions of fundamental masses and coupling constants,

$$\alpha^{\rm eff}(\boldsymbol{r}, t) = [1 + \Gamma_\alpha |\phi(\boldsymbol{r}, t)|^2]\alpha, \tag{2.3}$$

$$m_f^{\rm eff}(\boldsymbol{r}, t) = [1 + \Gamma_f |\phi(\boldsymbol{r}, t)|^2] m_f, \tag{2.4}$$

where m_f are the nominal values of fermion masses and α is the electromagnetic fine structure constant. The coupling constants Γ have units of $[\text{Energy}]^{-2}$ and we define the effective energy scales $\gamma_X \equiv 1/\sqrt{|\Gamma_X|}$ with $X = \alpha, m_f$.

The observable atomic frequency changes induced by DM objects can be linked to the variation of fundamental constants, and therefore the DM field parameter, described by Eqs. (2.3) and (2.4). For a particular clock transition,

$$\frac{\delta\omega(\boldsymbol{r}, t)}{\omega_0} = \sum_X \kappa_X \Gamma_X |\phi(\boldsymbol{r}, t)|^2 \equiv \Gamma_{\rm eff} |\phi(\boldsymbol{r}, t)|^2, \tag{2.5}$$

where ω_0 is the nominal clock frequency, X runs over relevant fundamental constants, and κ_X are dimensionless sensitivity coefficients. For convenience, we introduce the effective constant $\Gamma_{\rm eff}$ which depends on the specific clock type. Linear combinations of the coupling constants are noted in Refs. [11, 12].

This thesis focuses on the "thin" domain wall DM signal. It retains the main features of other more complicated types of DM "clumps", but gives an

analytically treatable signature. The basis of this signal model detailed more in Ref. [5]. Of important note is how we distinguish "thin" from "thick" signals based on sampling rate (which must be finite, of course). If interaction time with the device (the entire GPS constellation in this case) d/v_g is shorter than the sampling interval τ_0, then the exact arrival time of the DM clump is not resolved, nor is its shape. We then say it is "thin" for observational purposes when $d \ll v_g \tau_0$.

The value (in units of time) of the effective coupling relates to the maximum DM-induced clock phase signal accumulated $h = \delta\omega_{max}/\omega_0 \times \tau$ by

$$h = A^2 \Gamma_{\text{eff}} \tau, \tag{2.6}$$

$\tau = d/v_\perp$ being interaction time of a wall moving at velocity v through an individual device. Strictly speaking, for domain walls the relevant component of velocity is only the component normal to the wall, $v_\perp$. A "thin" wall requires that τ must be less than the sampling interval τ_0 [12].

Chapter 3

GPS.DM Project

The work of the GPS.DM group is to find DM using the GPS satellite constellation. The DM model of interest is self-interacting macroscopic objects such as TDs or Q-balls [12]. A DM constituent with a velocity according to the standard halo model [5] may pass through the GPS satellite constellation and feebly interact with the on-board clocks. This DM constituent may interact with standard model particles to change fundamental constants which then change the frequencies of atomic clocks. By searching for variations in the frequencies of atomic clocks it may be possible to sense the DM as a transient perturbation in the constellation [12].

Previous analysis done by the GPS.DM focused on finding large DM signals well above the instrument noise. Using the data publicly available by the Jet Propulsion Laboratory (JPL), new limits were placed on DM couplings that were orders of magnitude more stringent than previous astrophysical limits [8, 12]. No DM signatures were found, however. The next step, then, is to do the analysis for signals within the magnitude of instrument noise.

A desiderata of network sensors in Ref. [12] supports why the GPS constellation is used for this analysis, rather than a single atomic clock or multiple clocks of one satellite. Based on the standard halo model, a network of sensors detecting a DM object sweeping through at galactic velocities ($v_g \sim 300\,\mathrm{km/s}$)

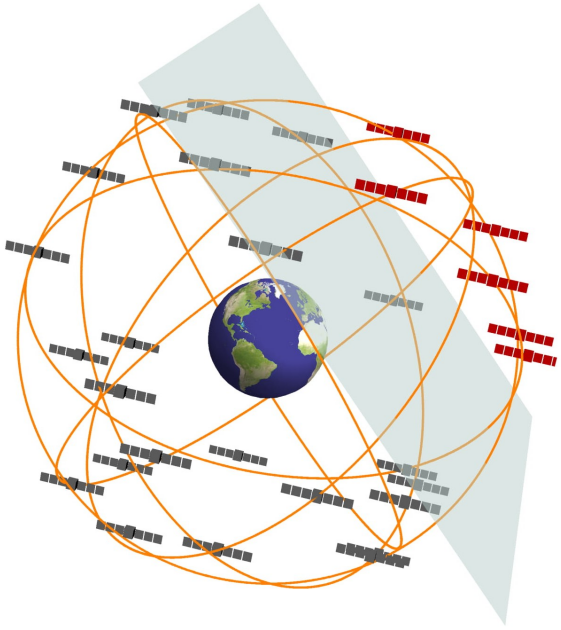

Figure 3.1: A visualization of a domain wall object passing through the GPS constellation. Red satellites are effected by the domain wall and experience a time bias compared to the gray satellites that the domain wall has yet to pass [5].

must have a sufficient sampling rate to track the propagation. This enables reconstruction of the geometry important to the matched-filter technique implemented by the GPS.DM group.

As stated in Ref. [12], the matched-filter technique (MFT) is used to approximate some value h of a DM signal hidden in GPS data using a signal to noise ratio (SNR) as a detection statistic. Basically, using a predefined signal shape from a model templates are made within a range of possible shapes for an unknown signal strength. One could think of the MFT as a technique that maximizes an overlap between the templates and the data stream. This maximization is done with the help of a matched-filter statistic, such as a SNR. However, it is not usually the value of the SNR alone that determines the level of overlap, but rather the value of the SNR compared to a threshold [12]. MFT is one of two methods that will be used to search for DM signals closer to instrument noise. The second method of Bayesian statistical analysis was previously done in Ref. [11] and is expanded upon hereon.

Chapter 4

Bayesian Statistical Analysis

Bayesian analysis is a powerful method in cases of model selection and parameter estimation. The fundamentals of the analysis involve taking some set of hypotheses H_i with data D and prior information from a proposition I and write the probability for this as $p(H_i|D, I)$ [13].

The probability can then be manipulated via Bayes' theorem to change perspectives,

$$p(H_i|D, I) = \frac{p(H_i|I)p(D|H_i, I)}{p(D|I)}, \tag{4.1}$$

where we now obtain prior information $p(H_i|I)$ that doesn't depend on D, with posterior information $p(H_i|D, I)$. The term $p(D|I)$ is the global likelihood for the entire set of hypotheses, and $p(D|H_i, I)$ [13].

Parameter estimation comes from creating a probability distribution function that is the posterior. That is to say, Bayesian analysis does not give a single value of what a tested parameter could be, instead it gives a range with a most likely candidate. We can also take a range of allowed values with a credible interval, defined by

$$\int_R d\theta\, p(\theta|D, M) = C, \tag{4.2}$$

where θ is the entire set of hypotheses and C is a probability content (e.g., C=.95 or 95%).

For GPS.DM, θ is the vector incident velocity of the TDM v, the incident time of arrival for the DM object t_0, and the amplitude of the signal in the bias data h. In this work we desire to find the credible interval for some nonzero value of a DM event's amplitude h, such that zero is not included in the range. A credible interval such as this would guarantee that an event has taken place within the GPS satellite clocks.

Chapter 5

Viewing Window Likelihoods

This begins with a model M we want to test. The model is an explanation for data, D_k, with a time window centered on epoch k. The epochs for this research are defined as 30 sec sampling intervals at which JPL calculates data. The time window itself contains a set of data from individual epochs. The posterior requires knowledge of the model, I, which is used for parameters other than our signal amplitude, h. From the set of all signal specific parameters θ implicit to D_k, we can express the marginalized posterior. This posterior is for a single time window and can be used as the likelihood for a posterior of multiple windows. This will be referred to as $W_k(h)$ for the likelihood of an event occurring (I will say a window is effected, or an event is 'caught' to keep the physical situation in mind) and $\overline{W}_j$ for an event not occurring

$$W_k(h) = p(D_k|M, I) = \int d\boldsymbol{\theta}\, p(\boldsymbol{\theta}|I)\mathcal{L}\left(D|h\, \boldsymbol{s}_k(\boldsymbol{\theta}), I\right) \tag{5.1}$$

$$\approx \sum_{i=1}^{N_{MC}} \mathcal{L}\left(D|h\, \boldsymbol{s}_k(\boldsymbol{\theta}_i), I\right)$$

$$\overline{W}_j = p(D_j|\overline{M}, I) = \mathcal{L}(D_j|h = 0, I)\,, \tag{5.2}$$

where the approximation is using the Monte Carlo numerical integration method. The term $\boldsymbol{s}_k(\theta)$ is a data template attempting to match to D. It is better shown in the second line where the Monte Carlo integration is indexed for the number of templates created to attempt a best match of D. The prior term disappears in the approximation due to inverse transform sampling. The method of inverse transform sampling is to take the inverse of a known distribution, in this case the prior, and use a uniformly spaced grid drawn through the known distribution to concentrate points to where the distribution is larger. In effect this will implicitly remove the prior as uniform points are transformed into points of the prior distribution [12]. We assume the likelihood to be a Gaussian distribution,

$$\mathcal{L}\left(D|h\,\boldsymbol{s}_{k_i}, I\right) = C_1 \exp\left[-\frac{1}{2}\left(\boldsymbol{d}_k - h\boldsymbol{s}_{k_i}\right)^T \boldsymbol{E}^{-1}\left(\boldsymbol{d}_k - h\boldsymbol{s}_{k_i}\right)\right], \tag{5.3}$$

where E^{-1} is the inverse covariance matrix, which determines the variances of clocks in relation to one another, and C_1 is a normalization constant. It will be written as $E^{-1} = H$ to save space. The vector $\boldsymbol{d}_k$ is the time bias data for a window centered on k, and $\boldsymbol{s}_{k_i}$ is the model predicted time bias data. The double index on $\boldsymbol{S}_{k_i}$ is to denote the number of templates i used in the Monte Carlo summation for a specific epoch k. Now consider the likelihood with substitutions,

$$\hat{h}_k = \frac{\boldsymbol{d}_k{}^T H \boldsymbol{s}_{k_i}}{\boldsymbol{s}_{k_i}{}^T H \boldsymbol{s}_{k_i}},$$
$$\sigma^2_{k_i} = \frac{1}{\boldsymbol{s}_{k_i}{}^T H \boldsymbol{s}_{k_i}},$$

where $\hat{h}_k$ is the signal strength that maximizes the likelihood and $\sigma^2_{k_i}$ is the template-specific likelihood variance. The likelihood term is now easily separable between the constant terms and the distribution term,

$$\mathcal{L}\left(D|h\,\boldsymbol{s}_{k_i}, I\right) = C_1 \exp\left\{-\frac{1}{2}\frac{(h-\hat{h_i})^2}{\sigma^2_{k_i}} + \frac{\hat{h_i}^2}{2\sigma^2_{k_i}} - \frac{d_k{}^T H d_k}{2}\right\}. \tag{5.4}$$

Thus the posterior is,

$$W_k(h) = C_2 \sum_{i=1}^{N_{MC}} \exp\left\{-\frac{1}{2}\frac{(h-\hat{h_i})^2}{\sigma^2_{k_i}} + \frac{\hat{h_i}^2}{2\sigma^2_{k_i}}\right\}, \tag{5.5}$$

where C_2 is the normalization which has also absorbed the second term in the exponential which is constant in respect to this sum.

In Ref.[12] there is brief discussion on the sensitivity of the search proportional to the number of windows considered. If the events are assumed to be Poisson distributed in time, then there is some average time between events $\mathcal{T}$. For the 20 years of archival GPS data there would be an expected number of events $N_E = (20\,\text{years})/\mathcal{T}$. Then if multiple windows are used add up to the total 20 year time spam and events are assumed to be non-overlapping, then the detection statistic for the matched-filter technique will increase by a factor of $\sqrt{N_E}$ while the variance remains the same. Therefore the sensitivity increases by the same factor of $\sqrt{N_E}$.

This increase in sensitivity is related to the work here. While Ref. [12] only makes note of this, the increase in time scale is the most important factor to potentially increasing the sensitivity of a search.

Chapter 6

Likelihood for a Time Series

Now to consider the posterior of multiple windows. $W_k(h)$ is the posterior for a single window, so the same expression will be used in multiple windows. The question is then how to combine multiple terms of $W_k(h)$. The options are taking the sum or product of every window. We need to consider what physical meaning each option has. A sum of all window probabilities will find the greatest probability from any present maximum. A product of all windows will find the greatest probability only if every window is at a maximum. From this, consider the product of all $W_k(h)$ shown also in Table (6.1),

$$W_1(h) * W_2(h) * W_3(h) * W_4(h) * \cdots * W_{N_W}(h)\,,$$
$$p^{N_W}(h|D,I) = C_3 \prod_{k=1}^{N_W} W_k(h)\,,$$

k	1	2	3	4	$\cdots$	N_W
A	✓	✓	✓	✓	$\cdots$	✓

Table 6.1: A window's centered epoch k along the columns, with the window set A for rows. The check marks reference which windows have events, in this table it is every window.

k	1	2	3	4	$\cdots$	N_W
A_1	✓	×	×	×	$\cdots$	×
A_2	×	✓	×	×	$\cdots$	×
			$\vdots$			
A_{N_W}	×	×	×	×	$\cdots$	✓

Table 6.2: A window's centered epoch along the columns and possible posterior distribution $W_k(h)$. A check mark is to reference where an event should be.

where p^{Nw} refers to the probability of N_W total windows containing an event. To say this is the posterior, it is necessary to consider every window contains an event because when this is not the case there are different combinations to test. Taking the sum of these various combinations will find the greatest probability for when at least one correctly matches the data.

Consider the simplest case, for when only one window in the time series catches an event. The event is not unique to which window is hit, so we check every possible window as if it were the only one effected. Referring to Table 6.2, the columns are still a product while the rows sum together, such that,

$$p^1(h|D,I) \propto A_1 + A_2 + \cdots + A_{N_W} ,$$
$$A_1 = W_1(h) * \overline{W}_2 * \overline{W}_3 * \overline{W}_4 * \cdots * \overline{W}_{N_W} ,$$
$$p^1(h|D,I) = C_3 \sum_k^{N_W} \left(W_k \prod_{j \neq k} \overline{W}_j \right) ,$$

where we are only looking at the posterior for a single window catching an event.

The next logical step is having an event present in two windows. It is important to understand how the combinations are represented. The product will include a second indexed $W(h)$ term. The sum now changes, as adding a second index will cause duplicate cases to pop out. This is easiest to understand as we are taking a combination, not a permutation. The difference being in a combination it does not matter which window is effected in which order, as there

k	1	2	3	$\cdots$	N_W-1	N_W
A_1	✓	✓	×	$\cdots$	×	×
A_2	✓	×	✓	$\cdots$	×	×
			$\vdots$			
A_{N_W}	×	×	×	$\cdots$	✓	✓

Table 6.3: The combinations available for two windows catching events.

is no physical order. The current model and analysis of GPS.DM assumes that only one DM event passes through the system, as only one event can be resolved for any window regardless of signal amplitude. Thus, one window cannot be effected by 'two' events[1]. To make this posterior a combination, consider one index kept lower than another for every step of the sum, $k_1 < k_2$,

$$p^2(h|D,I) \propto A_{1,2} + A_{1,3} + \cdots + A_{N_W-1,N_W} ,$$
$$A_{1,2} = W_1(h) * W_2(h) * \overline{W}_3 * \overline{W}_4 * \cdots * \overline{W}_{N_W} ,$$
$$p^2(h|D,I) = C_3 \sum_{k_1<k_2}^{N_W} \left(W_{k_1}(h) W_{k_2}(h) \prod_{j\neq k} \overline{W}_j \right) .$$

This posterior for two event windows has many more calculations compared to the single event window, but the general form the equation takes has only included one extra indexed term to the product and an index related by an inequality to the sum. At first it seems odd to use this inequality, but without it (say using an additional sum instead) there will be extra calculations that shouldn't exist. The indexed windows are in order of the epoch they're centered on, so it does not mean anything to order them differently for calculations.

This can easily be generalized to any specific number of windows n containing

[1]This posterior is specifically for two windows catching the event, so if a sum includes matching indices it would instead describe the previous case for a posterior of a single effected window.

an event,

$$p^n(h|D,I) = C_3 \sum_{k_1<k_2<\ldots<k_n}^{N_W} \left(\prod_{k_1,k_2,\ldots,k_n} W_k(h) \prod_{j\neq k} \overline{W}_j \right) . \tag{6.1}$$

It is important to remember that this posterior calculated is only a posterior of n specific windows catching an event. We can clean up the calculations by dividing through with the product of all $\overline{W}$ and absorbing the remnants in the normalization constant C_4,

$$p^n(h|D,I) = C_4 \sum_{k_1<k_2<\ldots<k_n}^{N_W} \left(\prod_{k_1,k_2,\ldots,k_n} \frac{W_k(h)}{\overline{W}_k} \right) . \tag{6.2}$$

Now to make a posterior for every possible number of effected windows, we sum through all n. Once again a sum is used to verify that any one of the possible combinations matches a tested value of h. Therefore, the posterior for an observation period is,

$$p(h|D,I) = C_5 \sum_{n=1}^{N_W} \left[\sum_{k_1<k_2<\ldots<k_n}^{N_W} \left(\prod_{k_1,k_2,\ldots,k_n} \frac{W_k(h)}{\overline{W}_k} \right) \right] . \tag{6.3}$$

To round this back to the work of the GPS.DM group, this calculation is directly doable for a small number of windows, but rapidly becomes too large to compute with increasing windows.

Chapter 7

Example Construction

Now that we have developed a statement for the posterior, we want to check expected results. We can do this by creating an example scenario where we make simplifying assumptions:

- There is one white noise clock
- There is no reference clock
- There is only one signal template

These assumptions will cause previous vector and matrix variables to be scalar. These include,

$$s = 1\,,$$
$$H = \frac{1}{\sigma^2}\,,$$
$$d_k = n_k + \sum_{q\in\{q\}} \tilde{h}\delta_{kq}\,.$$

Here s is normally the signal template which is a vector containing ones and zeros to correspond to clocks catching an event or not, so consider it to always be one. H is the inverse covariance matrix, but with only one clock it is simply

the inverse variance. From the assumption of a white noise clock, the term for noise contribution, n_k, will become an average of zero. The term $\sum_{q\in\{q\}} \tilde{h}\delta_{kq}$ refers to windows that contain events with the integer set $\{q\}$ specified by us. The sum is used to keep nonzero terms from the set $\{q\}$. The other variable of the sum, $\tilde{h}$, is the input signal's amplitude which we will also set ourselves.

Now we can apply this to Eq.(6.3). Only the weighted likelihood is changed,

$$\frac{W_k(h)}{\overline{W}_k} = \exp\left\{-\frac{h^2}{2\sigma^2}\right\} \exp\left\{\frac{h\sum_{q\in\{q\}} \tilde{h}\delta_{k,q}}{\sigma^2}\right\}, \tag{7.1}$$

where the previous variable changes are plugged into Eq.(5.1) and Eq.(5.2). Now to plug this into the posterior defined by Eq.(6.3). The posterior can now be solved analytically. This can be done by specifying windows to contain events. Let's start with only two windows, one of them being an event. The posterior will then be,

$$p(h|D,I) = C_5\left(\frac{W_1(h)}{\overline{W}_1} + \frac{W_2(h)}{\overline{W}_2}\right). \tag{7.2}$$

Plugging Eq.(7.1) into the previous line,

$$p(h|D,I) = C_5\left(\exp\left\{\frac{h\sum_q \tilde{h}\delta_{1,q}}{\sigma^2} - \frac{h^2}{2\sigma^2}\right\} + \exp\left\{\frac{h\sum_q \tilde{h}\delta_{2,q}}{\sigma^2} - \frac{h^2}{2\sigma^2}\right\}\right). \tag{7.3}$$

Since we set q, let's set it to $q = \{1\}$. This means that window one will have the event, while window two will not since it is not listed. Note that it does not matter which window was chosen. Now to clean up with this information,

$$p(h|D,I) = C_5 \exp\left[-\frac{h^2}{2\sigma^2}\right]\left(\exp\left[\frac{h\tilde{h}}{\sigma^2}\right] + 1\right). \tag{7.4}$$

It is apparent that the window without the event has become a value of 1 when factoring out the common exponential. It can be inferred that any extra time windows for this case will be the same, as only one event is placed into the observation period. Thus,

$$p(h|D,I) = C_5 \exp\left[-\frac{h^2}{2\sigma^2}\right]\left(\exp\left[\frac{h\tilde{h}}{\sigma^2}\right] + (N-1)\right), \tag{7.5}$$

where N is the total number of windows we are considering for the observation period. It is important to note that it does not matter which window contains

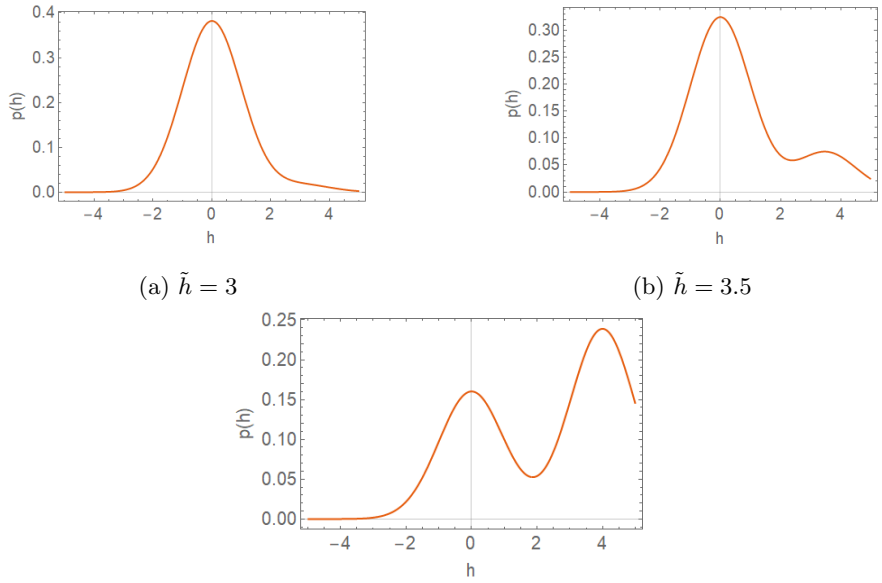

(a) $\tilde{h} = 3$

(b) $\tilde{h} = 3.5$

(c) $\tilde{h} = 4$

Figure 7.1: Normalized probabilities for increasing event amplitudes acting on a single window. The standard deviation and the total number of windows, $M = 2000$, are held constant.

the event. Since we set which window the event is in, we can assume to set it in only a single possible combination. This analytic answer of the posterior shows that a bimodal distribution is possible for values of $\tilde{h}$ proportionally greater than $(N - 1)$ with a diminishing factor of σ.

The next step for finding the posterior of arbitrary windows and events will come as a choice. I've ignored this for the last example, but when working through more than one possible window containing an event, there is a difference between the number of windows we are checking for to contain the event and how many events there actually are. This confusion comes from the product term, which we use to maximize the probability when more than one window has an event. We mildly cheat by setting q, but the product term will still run through different window numbers. Effectively, even when only one event is present, we check for more than there are, and the inverse also happening for

when many windows contain an event. This will result in something different from when we ourselves set $q = \{1, 2\}$ and then check for that case. So, let's see what happens if we test for more events than there really are,

$$p = C_5 \left(\frac{W_1(h)}{\overline{W}_1} \frac{W_2(h)}{\overline{W}_2} + \frac{W_1(h)}{\overline{W}_1} \frac{W_3(h)}{\overline{W}_3} + \frac{W_2(h)}{\overline{W}_2} \frac{W_3(h)}{\overline{W}_3} + ... \right) .$$

There are now two unique terms in the sum. First is where a window containing the event is multiplied by a window not containing the event. The second is when two windows without the event multiply. With $q = \{1\}$, the first unique term comes from the product window catching an event and a window without any interaction,

$$\begin{aligned} \frac{W_1(h)}{\overline{W}_1} \frac{W_2(h)}{\overline{W}_2} &= \exp\left[\frac{h \sum_q \tilde{h} \delta_{1,q}}{\sigma^2} - \frac{h^2}{2\sigma^2} \right] \exp\left[\frac{h \sum_q \tilde{h} \delta_{2,q}}{\sigma^2} - \frac{h^2}{2\sigma^2} \right] , \qquad (7.6) \\ &= \exp\left[-\frac{(h - \frac{\tilde{h}}{2})^2 - (\frac{\tilde{h}}{2})^2}{\sigma^2} \right] , \end{aligned}$$

while the second unique term is the product of two unaffected windows,

$$\begin{aligned} \frac{W_2(h)}{\overline{W}_2} \frac{W_3(h)}{\overline{W}_3} &= \exp\left[\frac{h \sum_q \tilde{h} \delta_{2,q}}{\sigma^2} - \frac{h^2}{2\sigma^2} \right] \exp\left[\frac{h \sum_q \tilde{h} \delta_{3,q}}{\sigma^2} - \frac{h^2}{2\sigma^2} \right] , \qquad (7.7) \\ &= \exp\left[-\frac{h^2}{\sigma^2} \right] . \qquad (7.8) \end{aligned}$$

Now the posterior for three windows will be,

$$p(h|D, I) = C_5 \left(2 \exp\left[-\frac{(h - \frac{\tilde{h}}{2})^2 - (\frac{\tilde{h}}{2})^2}{\sigma^2} \right] + \exp\left[-\frac{h^2}{\sigma^2} \right] \right) , \qquad (7.9)$$

where the coefficients of the exponential terms are simply the number of times an exponential term appears. Thus, the exponentials themselves will not change with the number of windows used but the coefficients will. So to expand the equation for any number of windows used, N,

$$\begin{aligned} p = C_5 \Bigg((N-1) \exp\left[-\frac{(h - \frac{\tilde{h}}{2})^2 - (\frac{\tilde{h}}{2})^2}{\sigma^2} \right] \\ + \left[\binom{N}{2} - (N-1) \right] \exp\left[-\frac{h^2}{\sigma^2} \right] \Bigg) . \qquad (7.10) \end{aligned}$$

Now consider labelling the number of events tested for Q. From the combinatorics of the $Q = 3$ case, it can be inferred that the posterior can be generalized as,

$$p^Q = C_5 \left\{ \binom{N-1}{Q-1} \exp\left[-\frac{Q[(h - \frac{\tilde{h}}{Q})^2 + (\frac{\tilde{h}}{Q})^2]}{2\sigma^2} \right] + \left[\binom{N}{Q} - \binom{N-1}{Q-1} \right] \exp\left[-\frac{Qh^2}{2\sigma^2} \right] \right\}, \quad (7.11)$$

for any value of Q. This can trivially be expressed as the sum of possible values for Q,

$$p = C_5 \sum_{Q=1}^{N} \left\{ \binom{N-1}{Q-1} \exp\left[-\frac{Q(h - \frac{\tilde{h}}{Q})^2 - (\frac{\tilde{h}}{Q})^2}{2\sigma^2} \right] + \left[\binom{N}{Q} - \binom{N-1}{Q-1} \right] \exp\left[-\frac{Qh^2}{2\sigma^2} \right] \right\}. \quad (7.12)$$

This posterior is defined for a single event placed amongst the windows in an observation period, but will not work for multiple events. Thus, the expression for multiple events needs to be derived similarly to the first. This starts with saying that there are now two events in the observation period, and that a meaningful value to test for is $Q = 2$ as it is the matching number,

$$\begin{aligned} \frac{W_1(h)}{\overline{W}_1} \frac{W_2(h)}{\overline{W}_2} &= \exp\left[\frac{h \sum_q \tilde{h} \delta_{1,q}}{\sigma^2} - \frac{h^2}{2\sigma^2} \right] \exp\left[\frac{h \sum_q \tilde{h} \delta_{2,q}}{\sigma^2} - \frac{h^2}{2\sigma^2} \right], \quad (7.13) \\ &= \exp\left[-\frac{(h - \tilde{h})^2 - (\tilde{h})^2}{\sigma^2} \right], \end{aligned}$$

where $q = \{1, 2\}$. It is desirable to note that a general exponential term can be made for the posterior at this point,

$$T(h) = \exp\left\{ -\frac{Q[(h - \frac{k\tilde{h}}{Q})^2 - (\frac{k\tilde{h}}{Q})^2]}{2\sigma^2} \right\}, \quad (7.14)$$

where k is the number of events actually present. Thus a general expression for the posterior is,

$$p(h|D, I) = C_5 \sum_{k,Q} A' \, T(h), \quad (7.15)$$

where A' is some function that expresses the combinatorics of the exponential terms. Solving for A' via a single sum is nontrivial, so instead consider a different approach to the problem where the exponential terms are separated.

So far, each posterior has been made by looking at a fixed number of actual events present and then varying the number of total windows. A different strategy then is to keep the total number of windows fixed and instead vary the number of actual events present. The posterior in every consideration is made up of some observation period containing a number of windows, N_W, and a number of windows containing events, l,

$$L_1, L_2, L_3, ..., L_l, B_{l+1}, B_{l+2}, ..., B_{N_W}$$

where L_k are windows containing events while n_k are windows without events. Each window is defined as,

$$L_k(h, \tilde{h}) = L(h, \tilde{h}) = \exp\left\{-\frac{1}{2}\frac{(h-\tilde{h})^2}{\sigma^2} + \frac{\tilde{h}^2}{2\sigma^2}\right\}, \tag{7.16}$$

$$B_k(h) = B(h) = \exp\left\{-\frac{1}{2}\frac{h^2}{\sigma^2}\right\}. \tag{7.17}$$

To combine these window expressions, consider summing through by values of l. As l increases, there will be more windows of L_k and less of B_k. For every case of l the two types of windows will be raised to their respective amounts and multiplied together. Now there are two sums with one nested in the other,

$$p(h|D, I) = C_5 \sum_{i=0}^{l} \left[\binom{l}{i} L(h, \tilde{h})^i \sum_{j=0}^{N_W - l} \binom{N_W - l}{j} B(h)^j \right]. \tag{7.18}$$

This is the end of the process to find the posterior in the example problem and it should be noted that the results from this final equation will not look unique compared to Eq.(7.5). Actual values can be put in to give results regardless of the number of event windows, total windows, tested positives and that is the main purpose of this example. Unfortunately, this example solution runs into a similar problem as the general solution Eq.(6.3) where a large number of windows will be computationally heavy. Specifically the computation becomes

massive when the number of event windows are comparable to the number of nonevent windows.

Chapter 8

Conclusion

Previous work done in Ref. [11] shows the work and results for Bayesian statistical analysis of GPS data to find an event amplitude. This previous analysis is only done on a single window, however. The goal here is to show the results of multiple windows processed together. As shown by Fig.(7.1) multiple windows will actually have a bimodal distribution, with one peak centered at the null hypothesis ($h = 0$) and the second peak centered at, the estimated event amplitude ($h \neq 0$). This means that further work could be done to separate these two nearly Gaussian distributions and take a real confidence interval on the event amplitude. Furthermore this theoretically works for any number of windows used, up to the total number of windows used in a day.

The major issue with this method is that it is highly unrealistic for such a number of windows, as it rapidly becomes computationally heavy. So overall the process of this work could be used across several windows at a time to sanity check the results of the SNR test performed as well as the posterior of a single window. If a multiple window posterior is generated for data containing a possible event and the distribution is clearly bimodal, then the estimated event signal amplitude will be more rigorously denoted as a transient effect with a velocity in line with the standard halo model. This is because the bimodality can be inferred as the event amplitude being high enough to split off from the

null hypthesis, and that the event amplitude also appeared for only an individual window. This may verify the possible event to be a domain wall TD as opposed to other exotic models or different dimensioned TD's.

Bibliography

[1] K. Nomura, A. Ito, J. Soda, *The European Physical Journal C* **2020**, *80*, DOI 10.1140/epjc/s10052-020-7990-y.

[2] L. Roszkowski, E. 3. Sessolo, S. Trojanowski, *Reports on progress in physics. Physical Society* **2018**, *81 6*, 066201.

[3] M. Schumann, *Journal of Physics G: Nuclear and Particle Physics* **2019**, *46*, 103003.

[4] D. J. 3sh, *Physics Reports* **2016**, *643*, Axion cosmology, 1–79.

[5] B. M. Roberts, G. Blewitt, C. Dailey, M. Murphy, M. Pospelov, A. Rollings, J. Sherman, W. Williams, A. Derevianko, *Nature Communications* **2017**, *8*, DOI 10.1038/s41467-017-01440-4.

[6] Y. Michimura, T. Fujita, S. Morisaki, H. Nakatsuka, I. Obata, Ultralight Vector Dark Matter Search with Auxiliary Length Channels of Gravitational Wave Detectors, **2020**.

[7] S. D. McDermott, S. J. Witte, *Physical Review D* **2020**, *101*, DOI 10.1103/physrevd.101.063030.

[8] A. Derevianko, M. Pospelov, *Nature Physics* **2014**, *10*, 933–936.

[9] A. Vilenkin, *Physics Reports* **1985**, *121*, 263–315.

[10] T. Kibble, *Physics Reports* **1980**, *67*, 183–199.

[11] B. Roberts, G. Blewitt, C. Dailey, A. Derevianko, *Physical Review D* **2018**, *97*, DOI 10.1103/physrevd.97.083009.

[12] G. Panelli, B. M. Roberts, A. Derevianko, *EPJ Quantum Technology* **2020**, *7*, DOI 10.1140/epjqt/s40507-020-00081-9.

[13] P. Gregory, *Bayesian Logical Data Analysis for the Physical Sciences: A Comparative Approach with Mathematica® Support*, Cambridge University Press, **2005**.